

CHARACTERIZING GLOBAL INTER-ANNUAL DUST REMOVAL AND DEPOSITION USING THERMAL EMISSION IMAGING SYSTEM (THEMIS) INFRARED DATA C. A. Wolfe¹, C. S. Edwards¹, S. Piqueux², J. Bapst², ¹Northern Arizona University, Flagstaff, AZ 86011, ²Jet Propulsion Laboratory, California Institute of Technology, Pasadena, CA 91109, cw997@nau.edu

Introduction: Dust is ubiquitous on Mars and is constantly altering the appearance of both the atmosphere and surface. Aside from modifying the overall look of the planet, dust plays a key role in a variety of atmospheric and surface processes. While the atmosphere of Mars typically contains dust throughout the year, atmospheric dust load varies considerably from season to season. The amount of dust in the atmosphere influences the degree to which solar and infrared radiation are absorbed and scattered, controlling the atmospheric temperature of Mars and thus global circulation patterns [1]. Globally, it is estimated that 2.9×10^{12} kg/yr of dust is exchanged between the surface and atmosphere of Mars [2], making dust transport one of the most dynamic and prevalent geological processes occurring on present-day Mars.

The observed Martian dust cycle depends heavily on the availability of mobile dust particles at the surface [3]. Dust is currently deposited uniformly throughout the equatorial region at a rate of $\sim 40 \mu\text{m}/\text{global storm}$, but over geologic timescales, the rate of accumulation may vary from 0 to $250 \mu\text{m}/\text{yr}$ due to changes in atmospheric conditions produced by orbital variations [4]. Dust deposited during global dust storms is generally observed to be removed from only dark, high thermal inertia regions, thus resulting in a net accumulation of dust in bright, low thermal inertia regions. Surface dust deposits are known to exist on Mars in at least the three low thermal inertia regions of Arabia, Tharsis, and Elysium [4]. Observational estimates of deposition rates in these regions range from a few to almost $50 \mu\text{m}/\text{yr}$ [5], assuming the dust was deposited uniformly.

Context: While variations of the surface albedo and spectral properties linked to dust deposition, transport, and removal are well documented [5] [6] [7] [8], a global scale quantification of surface dust fluxes between dust sources and sinks before, during, and after dust storms has not been carried out to date. Poor constraints on surface dust fluxes not only prevent Global Circulation Models (GCMs) from providing accurate results, but impedes any improvement of dust storm prediction and forecasting. This knowledge gap will be addressed by characterizing the fine-scale (~ 100 m) context for dust migration using THEMIS IR data. More specifically, we will quantify an upper limit on the amount of inter-annual dust (in μm) deposited or removed from a selection of geographical regions during different seasons and times of day, allowing tighter constraints to be placed on the activity of dust sources and sinks.

Methodology: The inter-seasonal/annual depletion and replenishment of surface dust reservoirs available for dust storm onset and growth leaves a measurable thermophysical signature (i.e. thermal inertia, albedo) that we will quantify and map to constrain the availability of surface dust through time. Image pairs are obtained by querying a variety of acquisition- and observational-based parameters stored in a database containing the entire global THEMIS IR dataset. This query returns a list of data product IDs for images acquired just before sunrise ($\leq 90^\circ$ incidence angle) at roughly the same season ($\leq 20^\circ L_S$) and same local time (≤ 1 hour), but different Mars years. Only image pairs that are well-calibrated and have a regional area overlap greater than 100 km^2 are considered.

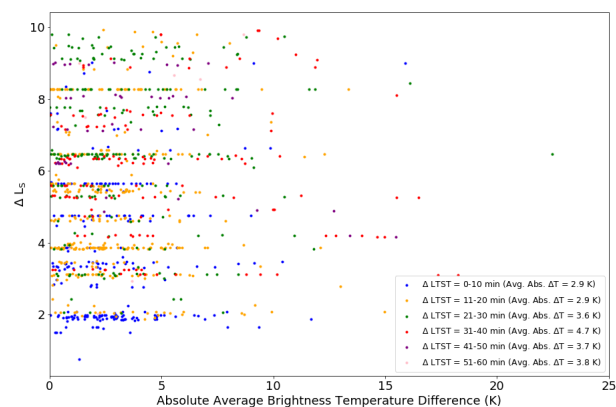


Figure 1: Absolute average brightness temperature difference as a function of L_S difference with colors indicating local time difference (in min.) between images.

After performing the query outlined above, images and relevant metadata are downloaded using Bayleef, a Python library for interfacing with the US Geologic Survey's (USGS) Inventory Service. Images are then processed to correct for instrument noise and other artifacts using the DaVinci software package, following well-established procedures outlined in [9]. After images have been processed, each unprojected image is cropped based on its latitude, returning a geometrically projected image that only spans the overlapping region, thus minimizing the amount of storage space needed and computational time required by ensuing steps.

Once images have been processed and cropped, they are registered to within 0.5 pixels (~ 50 m) using a tie-point and bundle adjustment method developed by the

Integrated Software for Imaging Spectrometers (ISIS) [10]. In this step, a control network produces ties (control points) from one image to another (control measures) through a sub-pixel registration algorithm to identify common ground points across each image within a pair. After valid control measures are established, a bundle adjustment routine generates new camera and spacecraft pointing information. This updated pointing information is then used to project the image pairs to their relevant locations on Mars, requiring no further adjustment or warping after the initial projection [9].

After the successful registration and projection of each image, image post-processing and brightness temperature conversion is performed using DaVinci. Only the Band 9 (centered at $12.57\ \mu\text{m}$) brightness temperature values are used for this investigation. At this wavelength surface emissivity is high (~ 0.99), atmospheric opacity is low, and the surface-atmosphere temperature contrast is high [9], resulting in a high signal-to-noise ratio for both daytime and nighttime data, and thus accurate surface brightness temperature values.

To properly identify the inter-annual variability present within the image pairs, a systematic method to reliably assess image-image variability was performed. After converting each pixel's spectral radiance to a brightness temperature, a variety of useful statistics are collected, including the minimum, maximum, average, and standard deviation brightness temperature difference. The location and number of pixels over specific thresholds is also obtained. To further help identify and characterize changes in brightness temperature that may be the result of either large- or small-scale thermophysical differences, the average normalized brightness temperature difference is computed for each image pair.

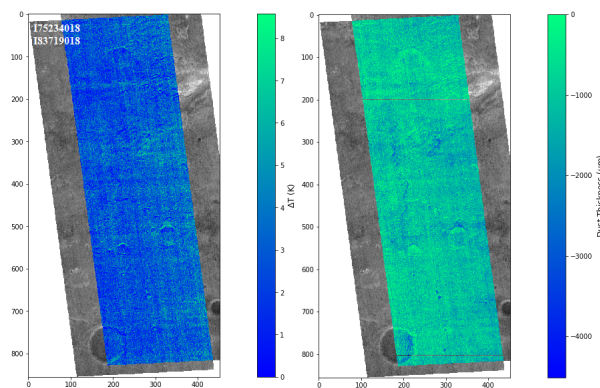


Figure 2: Brightness temperature difference (left) and modeled dust thickness change (right) for overlapping THEMIS image pair. Although both images depict relative uniformity, a closer inspection shows greater temperature differences in craters and river valleys, potentially corresponding to thicker layers of dust being removed.

Employing the KRC numerical thermal model [11], a variety of layered surface and subsurface conditions are simulated to produce a multi-dimensional lookup table. Specifically, we are interested in modeling the deposition/removal of a thin layer of fine-grained, low thermal inertia, high albedo dust particles on top a substrate with a higher bulk thermal inertia and lower albedo [12]. Using a host of input parameters, including L_S , latitude, local time, surface albedo, elevation, and dust opacity, surface temperature is derived for a variety of thermal inertia values, allowing different dust layer thicknesses to be modeled. By comparing modeled surface temperatures with observed values, an upper limit on the amount of dust deposited or removed from the overlapping region can be assigned to each image pair.

Preliminary Results: After applying the aforementioned criteria and a few additional constraints, the database query returned 1,071 image pairs that were successfully co-registered and bundle adjusted. The majority of these image pairs exhibit an average absolute brightness temperature difference of less than 15 K. As illustrated by Figure 1, a significant correlation does not appear to exist between average brightness temperature difference and season/local time difference. This is expected as keeping seasonal and local time differences between images small reduces the impact surface and subsurface heterogeneities may have on surface thermal inertia, and thus brightness temperature.

We have successfully demonstrated that dust removal and deposition at high spatial resolutions can be quantified from THEMIS IR brightness temperature differences using a linearly interpolated lookup table that links thermal inertia, brightness temperature difference, and dust layer thickness. Assuming albedo differences between images are small, the resulting dust thickness image places an upper limit on the amount of dust deposited or removed from a region formed by overlapping images. Figure 2 provides an example of brightness temperature difference being used to estimate the change in dust layer thickness. Here we see that depending on the thermal inertia of the surface, a brightness temperature difference increase between 2 and 4 K may correspond to a dust layer $\sim 1,100\ \mu\text{m}$ thick being removed.

References: [1] Ryan J.A. and Henry R.M., *JGR: Solid Earth*, 1979, [2] Pollack J.B. et al., *JGR*, 1977, [3] Kahre M.A. et al., *JGR: Planets*, 2006, [4] Christensen P.R., *JGR: Solid Earth*, 1986, [5] Christensen P.R., *JGR: Solid Earth*, 1988, [6] Vincendon M. et al. *Icarus*, 2015, [7] Wells E.N. et al., *Icarus*, 1984, [8] Szwast M.A. et al., *JGR: Planets*, 2006, [9] Edwards C.S. et al., *JGR: Planets*, 2011, [10] Gaddis L. et al., *LPSC*, 1997, [11] Kieffer H.H., *JGR: Planets*, 2013, [12] Edwards C.S. et al., *JGR: Planets*, 2011.